Available online at www.sciencedirect.com
ScienceDirect
Ceramics International 35 (2009) 13–20
CERAMICS INTERNATIONAL
www.elsevier.com/locate/ceramint

Two-step sintering of nanocrystalline $8Y_2O_3$ stabilized ZrO_2 synthesized by glycine nitrate process

Mehdi Mazaheri, M. Valefi, Z. Razavi Hesabi, S.K. Sadrnezhaad *

Materials and Energy Research Center, P.O. Box 14155-4777, Tehran, Iran

Received 27 June 2007; received in revised form 16 July 2007; accepted 2 September 2007
Available online 25 September 2007

Abstract

Two-step sintering was employed to consolidate nanocrystalline 8 mol% yittria stabilized zirconia processed by glycine-nitrate method. Results verified the applicability of this method to suppress the final stage of grain growth in the system. The grain size of the high density compacts (>97%) produced by two-step sintering method was seven times less than the pieces made by the conventional sintering technique. Up to ~96% increase in the fracture toughness was observed (i.e. from 1.61 to 3.16 MPa $m^{1/2}$) with decreasing of the grain size from ~2.15 to ~295 nm. A better densification behavior was also observed at higher compacting pressures.

Keywords: 8Y-FSZ; Two-step sintering; Nanocrystalline; Fracture toughness

1. Introduction

Interest in synthesis and sintering of nanocrystalline ceramics have recently grown due to the significant improvement in their properties as compared to the conventional coarser grain compacts. There are many methods for preparation of nanocrystalline powders. Examples are sol–gel [1], chemical vapor synthesis (CVS) [2,3], combustion synthesis [4] and hydrothermal processing [5]. Among different routes, combustion synthesis is known as the most energy efficient, low cost and high yield technique capable of producing single or multi component high-purity oxides [4].

Yittria stabilized cubic zirconia (YCSZ) possesses high oxygen ionic conductivity and chemical stability over a wide range of temperature and oxygen partial pressure. It is, therefore, a well-known candidate for applications such as manufacturing of oxygen sensor, development of solid oxide fuel cell and making membrane for separation of oxygen [6–10]. In contrast to the tetragonal zirconia, low fracture toughness restricts the use of cubic zirconia as an electrolyte because of premature fracture due to the thermal and mechanical stresses [11–13]. Grain refining is a promising route for simultaneous increase of mechanical strength and fracture toughness [14]. The decrease of the grain size below 100 nm leads to the formation of attractive nanostructured ceramics having superior electrical [7,15], thermal [16], optical [17] and mechanical properties [18]. In addition to these advantages, using nanopowder to fabricate nanocrystalline parts considerably enhances sinterability at lower temperatures rather than those of micrometric grains. An accelerated grain growth during densification of nanopowder is, however, reported deteriorating the advantages of nanostructured bulk materials [19]. Spark plasma sintering and hot pressing are two promising techniques for production of nanostructured ceramics [20,21]. Equipments of these methods are, however, too sophisticated and unavailable as well as very expensive. To fabricate nanocrystalline ceramics by pressure-less conventional sintering route, grain boundary migration has to be abated. The grain growth in this process can be controlled by two approaches: one is to prohibit grain growth by addition or dispersion of a second phase particles; the other is to control grain growth by a novel processing method called two-step sintering (TSS) technique.

Tekeli et al. [22–24] added Al_2O_3 and SiO_2 particles to hamper grain growth in cubic phase zirconia. They showed that the dispersion of a small amount ($\leq$1 wt%) of second phase can improve the densification and suppress the grain growth. With

* Corresponding author. Fax: +98 21 88773352.
E-mail addresses: mmazaheri@gmail.com (M. Mazaheri), sadrnezh@sharif.edu (S.K. Sadrnezhaad).

0272-8842/$34.00
doi:10.1016/j.ceramint.2007.09.009

increasing of the amount of the second phase, the densification would be degraded while the final grain size would be significantly decreased [13]. It was attributed to the formation of porosities located in the grain interior and along the grain boundaries. Another problem of using second phase particles was that the homogenous distribution of second phase grains in the matrix was extremely difficult. This could probably decrease the sintering rate by inducing tensile mean-stress developed by differential shrinkage characteristics between second phase particles and matrix grains [22]. Zirconia grains around the perimeter of the second phase particles were unable to contact with each other freely. This was another reason for decreasing of the sintering rate.

Chen et al. [25] and Lei and Zhu [26] added TiO_2 and Sc_2O_3, respectively. Though the grain growth can be hindered by the addition of dopants such as SiO_2, Al_2O_3 and SiC, insulating phases can also be formed. These phases can cause degradation of ionic conductivity [25]. Han et al. [7] have reported that as the YSZ grain size becomes smaller the thickness of the intergranular region decreases, too. Consequently, intergranular conductivity would increase. An enhancement of 1–2 orders of magnitude in the specific grain boundary conductivity for YSZ was observed after the grain size of solid electrolyte reduced to nanocrystalline range [27]. While the second phase particles were added to control grain size, these particles located at grain boundaries resulting in increasing of the grain boundary width deteriorating grain boundary conductivity. Seemingly, the addition of second phase causes technical problems for fabrication of uniform, dense and ultrafine structure without degradation of ionic conductivity.

Another way to control grain growth uses novel processing technique to tailor the microstructure. Recently, a two-step sintering method has been proposed to achieve the densification of ceramic bodies without significant grain growth in the final stage of sintering [28]. This method modifies the sintering regimes by high temperature firing followed by rapid cooling and low temperature soaking of the samples. To succeed in two-step sintering, a sufficiently high starting density should be obtained during the first step. When the density is greater than a critical value, the pores become subcritical and unstable against shrinkage which is induced by capillary action. These pores can be filled as long as grain boundary diffusion allows, even if the particle network is frozen as it is clearly in the second step. Mazaheri et al. [29] have suggested proper temperatures for first (T_1) and second stages (T_2) in two-step sintering to prohibit grain growth without degradation of densification. On the contrary, the inappropriate regime can serve no evolution in densification as well as no remarkable grain growth difference in comparison with normal sintering (NS) [29].

Han et al. [7] used TSS technique to control the grain growth of YSZ nanopowder synthesized by a liquid phase method. Laberty-Robert et al. [8] as well as Ghosh et al. [30] have also investigated the effect of two-step sintering on microstructure of yittria stabilized zirconia. Yu et al. [31] took the benefit of this technique for sintering of powder injection-molded zirconia parts.

In addition to 8YSZ, two-step sintering has been successfully conducted on ZnO [29], Ni–Cu–Zn ferrite [32], $BaTiO_3$ [32], Al_2O_3 [33,34] and liquid phase sintering of SiC [35] as well as doped ZnO varistors [36].

In this study, two-step sintering is applied on nanocrystalline 8YSZ synthesized by glycine-nitrate process to achieve a dense ultrafine structure. The sintering behavior and microstructural evolution during densification of normal and two-step sintering process are compared. A comparison is also made of the mechanical properties of the ceramic bodies made by TSS technique with those of the normally sintered ones.

2. Experimental procedure

Experiments consisted of synthesis, characterization, compaction, sintering and mechanical properties determination of 8YSZ samples according to the following methods.

2.1. Powder synthesis and characterization

Nanocrystalline 8 mol% yittria stabilized zirconia was synthesized via glycine-nitrate process in a muffle furnace using zirconyl nitrate ($ZrO(NO_3)_2{\cdot}6H_2O$) and yttrium nitrate ($Y(NO_3)_3{\cdot}6H_2O$) as sources of oxidants with the elemental stoichiometric coefficient $\Phi = 1.163$. Details of the processing method and the characteristics of as-synthesized particles were the same as those reported in Ref. [4].

In order to break the foamy agglomerates, the as-synthesized sheet-like nanocrystalline agglomerates were milled in a planetary ball mill. The milling was conducted in isopropanol medium using zirconia balls at rotational speed of 200 rpm. The milled powder was dried in air at 60 °C for 24 h. The morphology of the powder was investigated by scanning electron microscopy (Philips XL30, Netherlands) and transmission electron microscopy (Philips CM 200 FEG, Netherlands). The specific surface area of the powder was determined by Brunauer–Emmett–Teller (BET) technique (Micromeretics Gemini 2375, USA).

2.2. Compaction

The compressibility curve of the powder was determined by pressing the powder in a steel cylindrical die (10 mm diameter). The milled powder was uniaxially pressed at different pressures. After ejection of the compacts from the die, the green density of the pellets was measured by volumetric method. This method consisted of measuring weight and dimensions of the compacts by using an accurate balance (10^{-5} g) and a micrometer caliper (10^{-5} m).

2.3. Sintering

The green bodies were non-isothermally sintered with a heating rate of (1/12) °C s^{-1} up to 1500 °C without holding at the highest temperature. Two-step sintering was conducted on samples pressed at 600 MPa with relative density of about 48.5% with respect to the theoretical density (TD). At the first

step, pellets were heated up to the higher temperature of $T_1 = 1250\ ^\circ C$ with a heating rate of (1/12) $^\circ C\ s^{-1}$. They were then cooled down to the lower temperatures of $T_2 = 950$ and 1050 °C with a cooling rate of (5/6) $^\circ C\ s^{-1}$ and soaked for a prolonged time up to 20 h. The density of the sintered samples was measured according to Archimedes method. To investigate the grain growth both during sintering and after full densification, the sintered pellets were mechanically polished and thermally etched. The microstructure of the prepared samples was investigated by SEM (Philips XL30, Netherlands). The grain size of the sintered samples was determined by multiplying the average linear intercept by 1.56 [37]. For each specimen, 15 line segments were taken into account.

2.4. Mechanical properties and phase analyses

Hardness and fracture toughness were measured by indentation method for samples with minimum and maximum grain size. Indentation test was conducted on polished samples with a load of 5 kg held for 20 s. The hardness (H_v) was calculated from the diagonal length of the indentation determined by SEM observation using the following equation [13]:

$$H_V = \frac{1.854P}{d^2} \quad (1)$$

where P is the applied load and d is the mean value of the diagonal length. Fracture toughness (K_{IC}) was determined by measuring the crack length emanating the indentation center indicated by C in the following equation [38]:

$$K_{IC} = 0.0016\left(\frac{E}{H_V}\right)^{1/2}\left(\frac{P}{C^{3/2}}\right) \quad (2)$$

where E is the Young's modulus, H_V is the Vickers hardness and P is the load.

XRD analysis was performed using Cu Kα on sintered samples to distinguish cubic and tetragonal phases. A continuous step scanning XRD analysis was conducted in the 2θ range of 25°–33° at a scanning rate of $0.001^\circ\ s^{-1}$ using a PW3710-based Philips Diffractometer to investigate the existence of any major peaks associated with the monoclinic phase. The same procedure was used in a 2θ range of 71°–76° to determine the existence of the tetragonal phase.

3. Results and discussion

Experimental results indicated size, shape, compressibility, sinterability, phase stability and mechanical properties of the nanocrystalline 8YSZ.

3.1. Powder characterization

Because of larger surface area of finer powder, the progress of the sintering process accelerates even at low temperatures. However, the finer the particles, the higher the tendency to form agglomerates retarding the densification significantly [39,40].

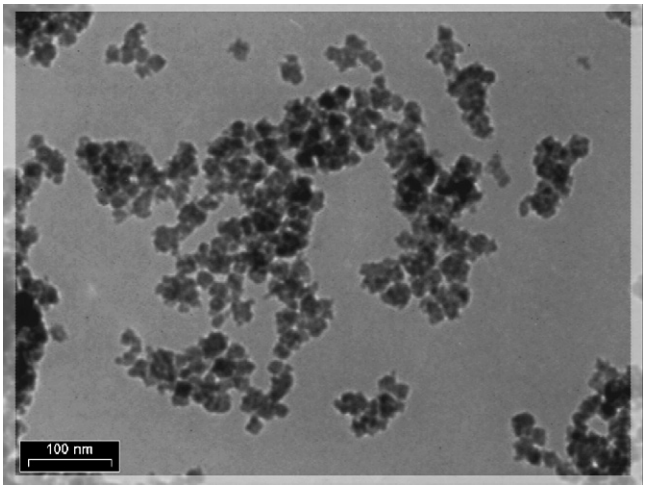

Fig. 1. TEM image of nanocrystalline 8YSZ powder synthesized via glycine-nitrate method after milling for 24 h.

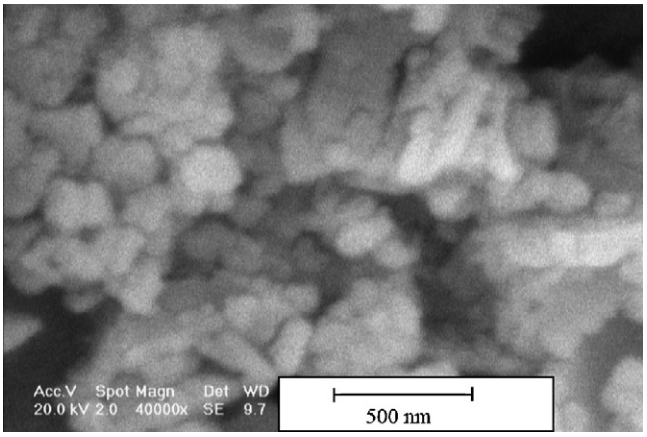

Fig. 2. SEM picture of milled nanocrystalline 8YSZ powder synthesized by glycine-nitrate process.

To regain a fine powder, one can grind the agglomerated pieces to obtain an easy-sintering feed. The powder formed during glycine-nitrate process was milled in this study to obtain the nearly spherical particles shown in Figs. 1 and 2. Results of BET test were used to determine the effect of milling on the surface area of the feed. The data revealed a nearly 55% increase in the surface area of the feed from 26.6 to 41.2 $m^2\ g^{-1}$ during milling. The latter corresponds to an average particle size of around 24.5 nm. The size of the milled powders shown in Fig. 1 is estimated to be around 15–33 nm, which is in good agreement with the BET result.

3.2. Compressibility and sinterability

Fig. 3 demonstrates the change of green and fired density of the samples as a function of the applied pressure. Both densities increased with increasing of the compaction pressure. Their increasing rate decelerated, however, with the compaction pressure until they finally reached to a nearly flat plateau. No obvious improvement in the densification was achieved with further escalation of the pressure. A green density increase of

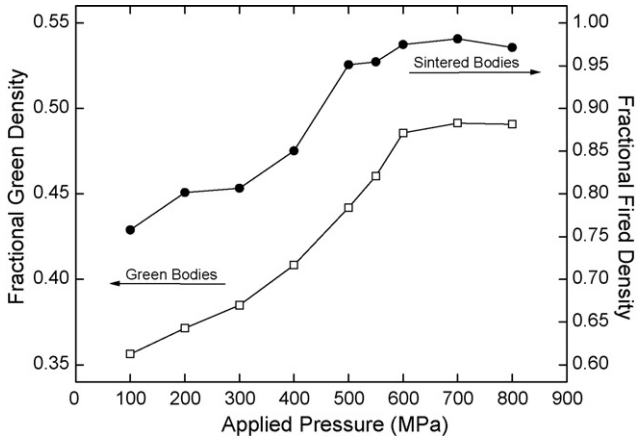

Fig. 3. Effect of applied pressure on relative green and fired density of nanocrystalline 8YSZ.

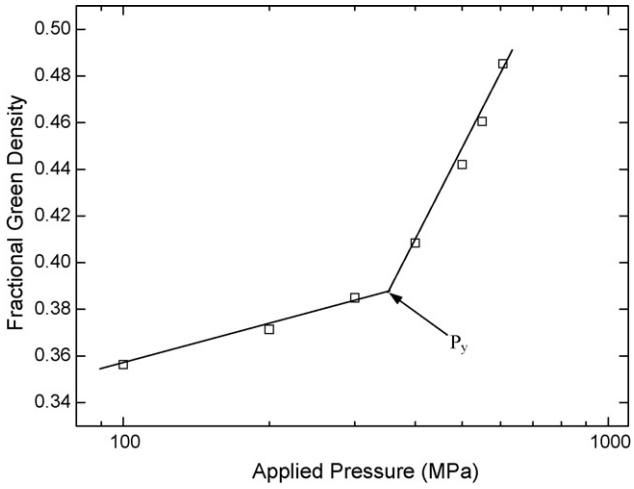

Fig. 4. Densification behavior of the milled nanocrystalline 8YSZ powder synthesized by glycine-nitrate process: P_y refers to agglomeration strength.

up to 38% with respect to the theoretical value was achieved by enhancement of the applied pressure from 100 to 800 MPa. Except 900 MPa which resulted in lamination in the samples, no lamination was generally observed at pressures applied to consolidate the milled powder in this research.

The consolidation behavior was influenced by size, morphology and size distribution of powders [41]. With decreasing of the particle size down to the nanorange, agglomeration of the nanoparticles became more feasible. Laberty-Robert et al. [8] previously reported that with increasing of the compaction pressure, green density increased up to a constant critical value. Their finding was the same as that of the present research. Sdric et al. [3] showed that the density increased with the logarithmic pressure. Li and Ye [33] reported a continuous density increase occurring as a function of the applied pressure.

Previous investigators considered the mechanism of consolidation of the ceramic-powders in a rigid die to include: (I) sliding and rearrangement of the particles; (II) fragmentation of brittle grains and (III) elastic deformation of bulk compacted powders [39]. At the early stage of compaction, restacking of the particles and rearrangement of the agglomerates dominated the mechanism of consolidation of the nanopowder. Further pressure rise leads to breakage of the weak agglomerates as well as the bridges formed during filling of the die [39,40]. In order to achieve higher density, extremely high pressure was needed to break the hard agglomerates.

Groot Zevert et al. [42] showed that in the case of the agglomerated powders, there was a turning point (P_y) in the plot of the relative density versus logarithm of the applied pressure, like that shown in Fig. 4. The curve was divided into two sharply separated linear parts with an interception at point P_y. The interception was called "strength of the agglomerates". After compaction at a pressure of around P_y, these agglomerates were gradually fragmented and then rearranged at lower pressures [42]. Fig. 4 shows the densification behavior of the milled nanocrytalline 8YSZ powder. It shows that the milling of the powder (prepared via glycine-nitrate process) resulted in partial breakage of the agglomerates.

Ghosh et al. [30] used the same method to determine the agglomeration strength of 8YSZ nanopowder produced via coprecipitation method. They showed that this method yielded a weak powder agglomeration with 80 MPa disintegration strength. The agglomeration strength of the powder used in this study was ~370 MPa. The source of the difference in compaction behavior of the powders might be the milling condition applied to the as-synthesized powder leading to the formation of finer particles. Ferkel and Hellmig [40] used mechanical milling to break agglomerates formed during nanopowder synthesis. They showed that mechanical milling significantly improved compressibility of alumina nanopowder.

Measurement of the fired density of the powder compacted at different pressures shows the effect of compressibility on densification due to sintering. The sintered density of the bodies fired in a furnace whose temperature rising up to 1500 °C with a constant heating rate of (1/2) °C s^{-1} showed that the powder compacted at higher pressures had a better densification behavior (Fig. 3). Fig. 5 shows the effect of green density on the fired density. A linear relationship was observed: the higher the green density, the greater the sintered density. This was due to the smaller size of the pores in the green bodies which could be

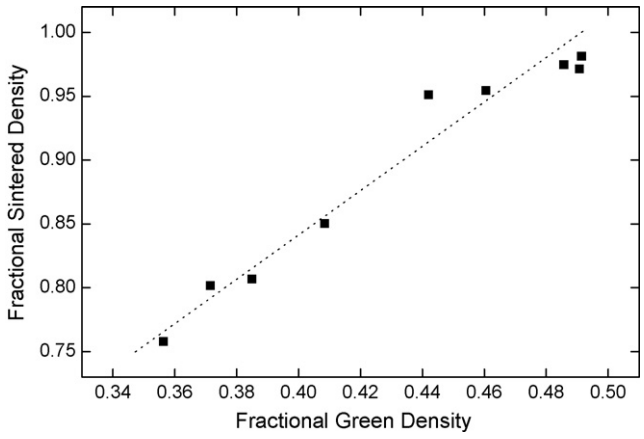

Fig. 5. Dependency of fired density on green density. Note that the green bodies were heated up to 1500 °C with a constant heating rate of (1/12) °C s^{-1} for their nonisothermal sintering without being held at the highest temperature.

removed during sintering. Similar findings were reported by Ferkel and Hellmig [40] and Gaudon et al. [43]. Based on the results of this study, the powder pressed at pressure ≥600 MPa became nearly fully-densed without dwelling at 1500 °C.

3.3. Conventional versus two-step sintering

To investigate the densification behavior and grain growth of the nanocrystalline powder during sintering, the grain size at different stages of sintering could be measured. It was well known that the decrease of the particle size and the increase of the surface area improved sinterability in the freely agglomerated powders. In case of nanopowders, accelerated grain growth was reported by many researches [7,29–31]. According to the thermodynamics laws, the effects of particle/crystallite size (d) on the intrinsic driving force ΔE_s (superfluous surface energy) of sintering was estimated by [44]:

$$\Delta E_s = \gamma_{sv} W_m S_p = 6 \times 10^3 \frac{\gamma_{sv} W_m}{\rho_{th} d} \quad (3)$$

where γ_{sv} was the surface energy of gas–solid interface (J m^{-2}), W_m was the molecular weight (g mol^{-1}), S_p was the specific surface area (m^2 g^{-1}) and ρ_{th} was the theoretical density of the solid solution oxide (g cm^{-3}). The smaller the starting particle size, the larger the specific surface area and the higher the driving force for densification.

Fig. 6 shows the changes of the fractional density and grain size versus the fired temperature after normal sintering (NS). The density versus temperature plot exhibited a sigmoidal shape. As seen, the sintering rate below 1150 °C was slow. The rate of densification increased drastically at 1250 °C and a significant densification was obtained at about 1350 °C. As a consequence, the increase of temperature from 1150 to 1300 °C increased the fractional density from 0.72 to 0.92 of TD. With further increasing of the sintering temperature (e.g. to 1500 °C), a relatively slight increase was obtained in the density. The change of grain size as a function of sintering temperature presents two distinct regions. At the first region, starting at 950 °C and continuing up to 1250 °C, the rate of grain growth was slow in which the grain size increased from 51 to 199 nm with increasing of the temperature from 950 to 1250 °C. In the second stage of sintering (usually between 0.65–0.9 TD), according to the solid state sintering mechanism, dispersed open pores could pin grain boundaries and hinder grain-boundary migration, for which the grain growth was suppressed. Second region was related to temperatures higher than 1300 °C. In this region, the final grain size of the sintered samples was sharply increased. When temperature increased from 1300 to 1500 °C, the grain size increased, for instance, from ~423 nm to 2.15 μm. It shows a significant grain growth at the final stage of sintering happening at 1500 °C. It was confirmed that the open pores (referring to the intermediate stage of sintering) collapsed to form closed pores, after which the final stage of sintering started (fractional density > 0.9). Such a collapse resulted in a substantial decrease in pore pinning, which triggers the accelerated grain growth.

In order to suppress the grain growth at final sintering stage, two-step sintering technique was applied. The results of two different regimes were presented in Fig. 7. First regime was carried out under following condition: T_1 = 1250 °C and T_2 = 950 °C (TSS_1) as well as second regime T_1 = 1250 °C and T_2 = 1050 °C (TSS_2). Mazaheri et al. [29] reported that for nanocrystalline ZnO, there was a critical temperature for second step to gain a fully dense structure without accelerated grain growth. At temperatures lower than that, even after long term holding time no improvement in densification could be gained. In other words, two-step sintering carried out at second step temperature (T_2) lower than the critical one turned out to be a disappointing process. They reported that surface diffusion contributed to grain growth without densification at temperatures lower than critical one [29]. A noticeable grain growth coincided, therefore, to the densification exhausts. Chen and Wang [28] confirmed that the reason for exhaustion of densification in the second step was attributed to the low temperature (T_2) which retarded grain boundary diffusion as the sintering mechanism. Similar results were obtained from the present work. Under TSS_1 sintering regime (T_1 = 1250 °C and T_2 = 950 °C) with prolonged soaking at 950 °C (up to 20 h), no

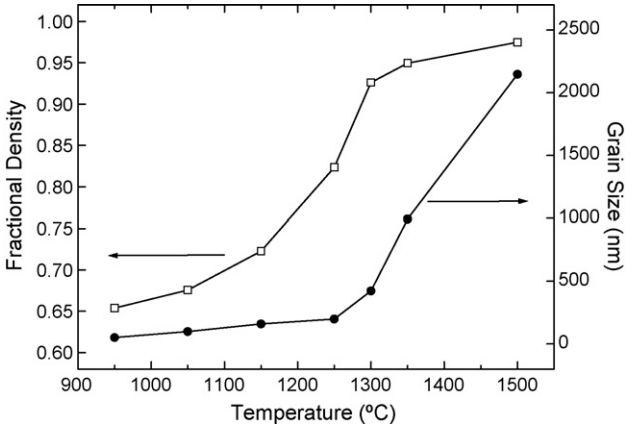

Fig. 6. Fractional fired density and grain size of nanocrystalline 8YSZ compacts as a function of sintering temperature under NS condition.

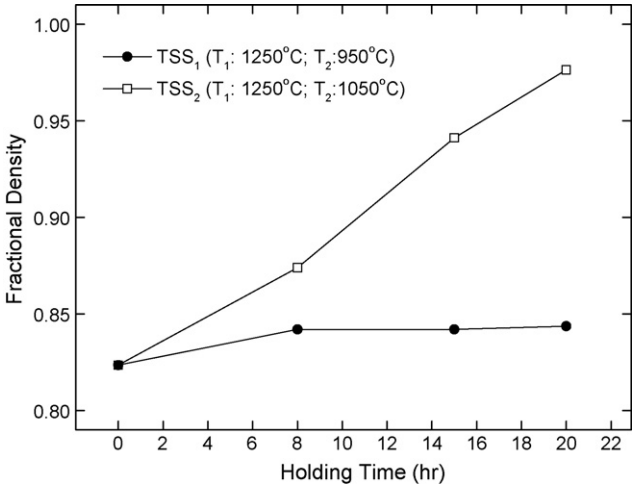

Fig. 7. Fractional density versus holding time at 950 and 1050 °C for nanocrystalline 8YSZ compacts sintered according to TSS_1 and TSS_2 regimes.

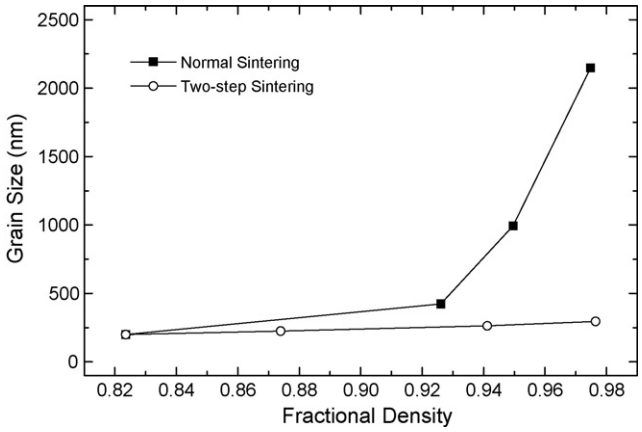

Fig. 8. Average grain size versus fractional density of nanocrystalline 8YSZ compacts sintered according to TSS_2 and NS regimes.

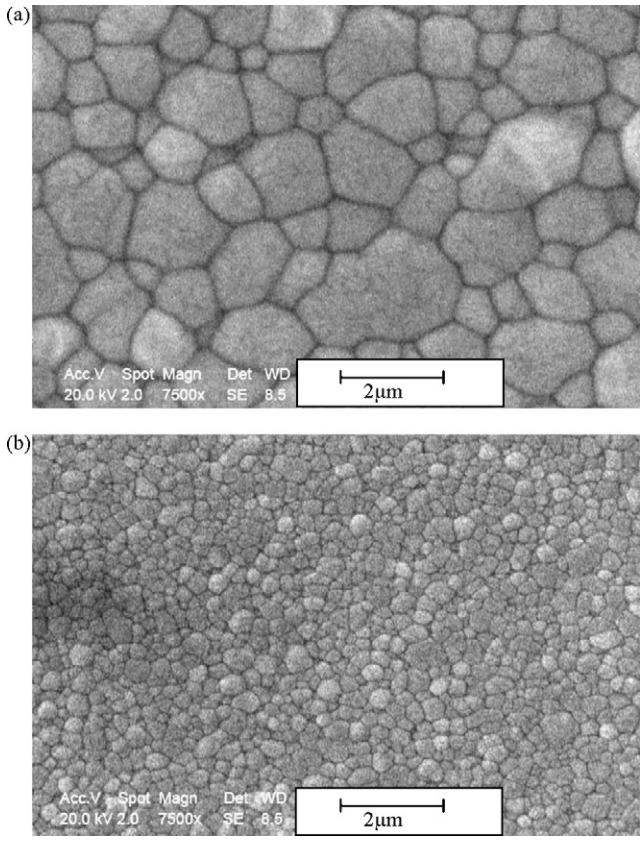

Fig. 9. SEM micrographs of nanocrystalline 8YSZ compacts sintered according to (a) NS and (b) TSS_2 regimes.

tangible variation in density was observed (see Fig. 7). In other words, densification occurred only when the distances between the centers of the crystallites was diminished. Such decrease needed an off-transport of matter from the grain boundaries to the neck. This was, of course, impossible without volume and grain boundary diffusion. At this temperature, densification mechanisms such as grain-boundary and volume diffusion were not active; so densification was exhausted [29]. In contrast, under TSS_2 regime (T_1 = 1250 °C and T_2 = 1050 °C) nearly full dense structure was obtained (see Fig. 7). On the base of the results of TSS_2 regime, the critical density making pores unstable at the end of the first step was around 82% of TD.

The result of TSS_2 process highlighted the role of this novel technique on grain growth. Soaking of the samples at T_2 (1050 °C) leads to a significant densification (from ~0.82 to ~0.98), while no significant increase occurred in the grain size (see Fig. 8). Fig. 9 shows the SEM pictures of the fully dense 8YSZ after sintering under normal and two-step sintering process. A considerable reduction in grain growth was observed. Yet the accelerated grain growth in the final stage of NS was of nature of this method. Chen and co-workers [19] explained that to achieve densification without grain growth, grain boundary diffusion needed to remain active, while the grain boundary migration had to be suppressed. A mechanism to inhibit grain boundary movement was a triple-point (junction) drag. Consequently, to prevent the accelerated grain growth, it was essential to decrease grain boundary mobility. The grain growth entailed a competition between grain-boundary mobility and the junction mobility. Once the latter became less at low temperatures in which junctions were rather immobile, the mentioned drag would occur. The grain growth was, therefore, prohibited under that condition. This grain boundary diffusion accompanied by triple point drag at low temperatures (T_2), contributed to a fully dense microstructure with a constant grain size.

3.4. Mechanical property and phase stability

In order to achieve better mechanical strength and improve toughness of ceramics, one could use grain refining mechanism [14]. Although in tetragonal zirconia reduction of grain size down to nanometer range made the transformation toughening difficult to occur leading to decrease of the fracture toughness [45], in cubic phase zirconia a significant increase in toughness was reported. For instance, Chen et al. [25] added TiO_2 dopant to control grain growth of 8YSZ during sintering. The grain size of undoped and 10 wt% TiO_2 doped 8YSZ was ~2.7 and ~1.2 μm, respectively, resulting in increase of the fracture toughness from 1.2 to 3.3 MPa $m^{1/2}$. Formation of small tetragonal grains and reduction of grain size were reported to be responsible for increase of the fracture toughness in this system [25]. However, the improvement of the fracture toughness by the addition of TiO_2 was accompanied by densification retardation. Tekeli [11] reported that the fracture toughness of undoped 8YSZ was about 1.5 MPa $m^{1/2}$, while the addition of 10 wt% Al_2O_3 particles increased the fracture toughness to 2.4 MPa $m^{1/2}$. In the present study, without the addition of any dopant, the grain size was decreased from 2.15 μm to 295 nm due to two-step sintering process without any deterioration of the densification. Consequently, the fracture toughness was increased from 1.61 to 3.16 MPa $m^{1/2}$ (Table 1). Ghosh et al. [30] reported a higher fracture toughness of about 3.5 MPa $m^{1/2}$ for 8YSZ sintered bodies even with coarser structures. The toughness values reported in the literature for fully stabilized zirconia were often in the range of 1.0–3.2 MPa $m^{1/2}$ depending on the microsturctural features [11,13,25,46,47]. The larger the grain size, the lower the fracture toughness. For coarse

Table 1
Mechanical properties of nanocrystalline 8YSZ compacts sintered according to NS and TSS_2 regimes

Sintering method	Fractional density	Grain size (μm)	Hardness (GPa)	Fracture toughness (MPa $m^{1/2}$)
Normal	97.5	2.15	12.87	1.61
TSS_2	97.6	0.295	13.51	3.16

structures having micrometric grain size, the fracture toughness obtained by most researchers was below 2 MPa $m^{1/2}$, while a significantly higher toughness value was reported even for a structure containing micrometer grains (<10 μm) by the former authors [30]. Annealing treatment applied before indentation test might enhance the crack propagation resistance by removing the surface defects.

To reveal the dominant mechanism of the toughening process, the crystal structure of the samples was investigated by XRD technique. X-ray diffraction analysis showed that the microstructure of both normally sintered and two-step sintered bodies only composed of a cubic phase (Fig. 10). In other words, in contrast to the results obtained by Chen et al. [25] indicating the formation of small tetragonal grains embedded in cubic structure, in the present study no transformation occurred with the reduction of particle size via TSS. The hardness of sintered samples also increased with reduction of the grain size. It was noticeable that with addition of 10 wt% TiO_2 to 8YSZ, no change was observed in hardness [25]. This can be attributed to lower density of doped 8YSZ relative to that of un-doped zirconia. The measurement of mechanical properties in the present study indicated, therefore, that with the reduction of grain size via two-step sintering process, not only did the fracture toughness increase but also the hardness enhancement occurred. Uniform ultra fine-grained microstructure of dense cubic zirconia phase obtained in this study was a promising candidate for SOFC application at lower temperatures.

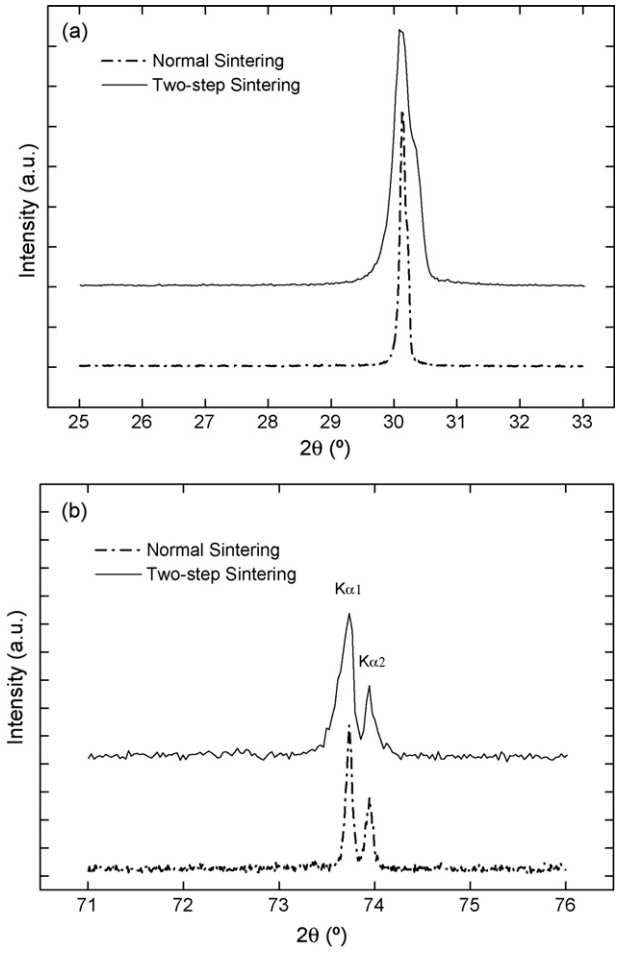

Fig. 10. Long-time XRD patterns of nanocrystalline 8YSZ compact sintered according to TSS_2 regime with the 2θ angle range of: (a) 25°–32° and (b) 71°–76°.

4. Conclusions

Nanocrystalline 8YSZ powder was synthesized using a modified glycine-nitrate process. The microstructure evolution during normal and two-step sintering was investigated. Hardness and fracture toughness of nearly full-dense structures obtained by different sintering regimes were measured. The following results were obtained:

1. Two-step sintering conducted at $T_1 = 1250\ ^\circ C$ and $T_2 = 1050\ ^\circ C$ significantly prohibited the grain growth in the final stage of sintering without deteriorating the densification process. At a lower second-step temperature (i.e. $T_2 = 950\ ^\circ C$), no densification was observed even after a prolonged soaking treatment.
2. The grain size was decreased from 2.15 μm (for normal sintering) to 295 nm by applying two-step sintering process.
3. A grain-size decreasing of up to 86% resulted in a fracture toughness increase of up to 96%.

Acknowledgement

Sincere appreciation must be made to Dr. A. Simchi of Sharif University of Technology for his useful advice. The authors, also, appreciate the very helpful companion of Mr. Abdolhamid Rezaie for taking the SEM micrographs.

References

[1] C. Suciu, L. Gagea, A.C. Hoffmann, M. Mocean, Sol–gel production of zirconia nanoparticles with a new organic precursor, Chem. Eng. Sci. 61 (2006) 7831–7835.
[2] V.V. Srdi, M. Winterer, Comparison of nanosized zirconia synthesized by gas and liquid phase methods, J. Eur. Ceram. Soc. 26 (2006) 3145–3151.
[3] V.V. Srdic, M. Winterer, H. Hahn, Sintering behavior of nanocrystalline zirconia prepared by chemical vapor synthesis, J. Am. Ceram. Soc. 83 (2000) 729–736.
[4] M. Valefi, C. Falamaki, T. Ebadzadeh, M. Solati-Hashjin, New insights of the glycine-nitrate process for the synthesis of nano-crystalline 8YSZ, J. Am. Ceram. Soc. 90 (2007) 2008–2014.

[5] K.G. Kanade, J.O. Baeg, S.K. Apte, T.L. Prakash, B.B. Kale, Synthesis and characterization of nanocrystallined zirconia by hydrothermal method, Mater. Res. Bull. (2007), in press.
[6] X.M. Wang, G. Lorimer, P. Xiao, Solvothermal synthesis and processing of yttria-stabilized zirconia nanopowder, J. Am. Ceram. Soc. 88 (2005) 809–816.
[7] M. Han, X. Tang, H. Yin, S. Peng, Fabrication, microstructure and properties of a YSZ electrolyte for SOFCs, J. Power Sources 165 (2007) 757–763.
[8] C. Laberty-Robert, F. Ansart, C. Deloget, M. Gaudon, A. Rousset, Dense yttria stabilized zirconia: sintering and microstructure, Ceram. Int. 29 (2003) 151–158.
[9] Q. Zhu, B. Fan, Low temperature sintering of 8YSZ electrolyte film for intermediate temperature solid oxide fuel cells, Solid State Ionics 176 (2005) 889–894.
[10] K. Prabhakaran, M.O. Beigh, J. Lakra, N.M. Gokhale, S.C. Sharma, Characteristics of 8 mol% yttria stabilized zirconia powder prepared by spray drying process, J. Mater. Process. Technol. 189 (2007) 178–181.
[11] S. Tekeli, Influence of alumina addition on grain growth and room temperature mechanical properties of 8YSCZ/Al_2O_3 composites, Compos. Sci. Technol. 65 (2005) 967–972.
[12] A.N. Kumar, B.F. Sorensen, Fracture energy and crack growth in surface treated yttria stabilized zirconia for SOFC applications, Mater. Sci. Eng. A333 (2002) 380–389.
[13] S. Tekeli, Fracture toughness (K_{IC}), hardness, sintering and grain growth behavior of 8YSCZ/Al_2O_3 composites produced by colloidal processing, J. Alloys Compd. 391 (2005) 217–224.
[14] A. Krell, P. Blank, The influence of shaping method on the grain size dependence of strength in dense submicrometer alumina, J. Eur. Ceram. Soc. 16 (1996) 1189–1200.
[15] L. Gao, Q. Li, W. Luan, Preparation and electric properties of dense nanocrystalline zinc oxide ceramics, J. Am. Ceram. Soc. 85 (2002) 1016–1018.
[16] H.S. Yang, G.R. Bai, L.J. Thompson, J.A. Eastman, Interfacial thermal resistance in nanocrystalline yittria-stabilized zirconia, Acta Mater. 50 (2002) 2309–2317.
[17] J. Wang, L. Gao, Photoluminescence properties of nanocrystalline ZnO ceramics prepared by pressureless sintering and spark plasma sintering, J. Am. Ceram. Soc. 88 (2005) 637–639.
[18] B.A. Cottom, M.J. Mayo, Fracture toughness of nanocrystalline ZrO_2–3 mol% Y_2O_3 determined by Vickers indentation, Scripta Mater. 34 (1996) 809–814.
[19] X.H. Wang, P.L. Chen, I.W. Chen, Two-step sintering of ceramics with constant grain-size, I. Y_2O_3, J. Am. Ceram. Soc. 89 (2006) 431–437.
[20] Y. Lee, J.H. Lee, S.H. Hong, D.Y. Kim, Preparation of nanostructured TiO_2 ceramics by spark plasma sintering, Mater. Res. Bull. 38 (2003) 925–930.
[21] A. Weibel, R. Bouchet, R. Denoyel, P. Knauth, Hot pressing of nanocrystalline TiO_2 (anatase) ceramics with controlled microstructure, J. Eur. Ceram. Soc. 27 (2007) 2641–2646.
[22] S. Tekeli, U. Demir, Colloidal processing, sintering and static grain growth behavior of alumina-doped cubic zirconia, Ceram. Int. 31 (2005) 973–980.
[23] S. Tekeli, M. Erdogan, B. Aktas, Microstructural evolution in 8 mol% Y_2O_3-stabilized cubic zirconia (8YSCZ) with SiO_2 addition, Mater. Sci. Eng. A386 (2004) 1–9.
[24] S. Tekeli, M. Guru, Microstructural design and high temperature tensile deformation behaviour of 8 mol% yttria stabilized cubic zirconia (8YCSZ) with SiO_2 additions, Ceram. Int. (2006), in press.
[25] T. Chen, S. Tekeli, R.P. Dillon, M.L. Mecartney, Phase stability, microstructural evolution and room temperature mechanical properties of TiO_2 doped 8 mol% Y_2O_3 stabilized ZrO_2 (8Y-CSZ), Ceram. Int. (2006), in press.
[26] Z. Lei, Q. Zhu, Low temperature processing of dense nanocrystalline scandia-doped zirconia (ScSZ) ceramics, Solid State Ionics 176 (2005) 2791–2797.
[27] P. Mondal, A. Klein, W. Jaegermann, H. Hahn, Enhanced specific grain boundary conductivity in nanocrystalline Y_2O_3-stabilized zirconia, Solid State Ionics 118 (1999) 331–339.
[28] I.W. Chen, X.H. Wang, Sintering dense nanocrystalline oxide with-out final stage grain growth, Nature 404 (2000) 168–171.
[29] M. Mazaheri, A.M. Zahedi, S.K. Sadrnezhaad, Two-step sintering of nanocrystalline ZnO compacts: effect of temperature on densification and grain growth, J. Am. Ceram. Soc.,in press.
[30] A. Ghosh, A.K. Suri, B.T. Rao, T.R. Ramamohan, Low-temperature sintering and mechanical property evaluation of nanocrystalline 8 mol% yttria fully stabilized zirconia, J. Am. Ceram. Soc. 90 (2007) 2015–2023.
[31] P.C. Yu, Q.F. Li, J.Y.H. Fuh, T. Li, L. Lu, Two-stage sintering of nanosized yttria stabilized zirconia process by powder injection molding, J. Mater. Process. Technol. (192–193) (2007) 312–318.
[32] X.H. Wang, X.Y. Deng, H.L. Bai, H. Zhou, W.G. Qu, L.T. Li, I.W. Chen, Two-step sintering of ceramics with constant grain-size, II: $BaTiO_3$ and Ni–Cu–Zn ferrite, J. Am. Ceram. Soc. 89 (2006) 438–443.
[33] J. Li, Y. Ye, Densification and grain growth of Al_2O_3 nanoceramics during pressureless sintering, J. Am. Ceram. Soc. 89 (2006) 139–143.
[34] K. Bodisova, P. Sagalik, D. Galusek, P. Svancarek, Two-stage sintering of alumina with submicrometer grain size, J. Am. Ceram. Soc. 90 (2007) 330–332.
[35] Y.I. Lee, Y.-W. Kim, M. Mitomo, D.Y. Kim, Fabrication of dense nanostructured silicon carbide ceramics through two-step sintering, J. Am. Ceram. Soc. 86 (2003) 1803–1805.
[36] P. Duran, J. Tartaj, C. Moure, Fully dense, fine-grained, doped zinc oxide varistors with improved nonlinear properties by thermal processing optimization, J. Am. Ceram. Soc. 86 (2003) 1326–1329.
[37] M.I. Mendelson, Average grain size in polycrystalline ceramics, J. Am. Ceram. Soc. 52 (1969) 443–446.
[38] G.R. Anstis, P. Chantikul, B.R. Lawn, D.B. Marshall, A critical evaluation of indentation techniques for measuring fracture toughness: I, direct crack measurements, J. Am. Ceram. Soc. 64 (1981) 533–543.
[39] P. Bowen, C. Carry, From powders to sintered pieces: forming, transformations and sintering of nanostructured ceramic oxides, Powder Technol. 128 (2002) 248–255.
[40] H. Ferkel, R.J. Hellmig, Effect of nanopowder deagglomeration on the densities of nanocrystalline ceramic green bodies and their sintering behavior, Nanostruct. Mater. 11 (1999) 617–622.
[41] O.L. Khasanov, E.S. Dvilis, V.M. Sokolov, Compressibility of the structural and functional ceramic nanopowders, J. Eur. Ceram. Soc. 27 (2007) 749–752.
[42] W.F.M. Groot Zevert, A.J.A. Winnubst, G.S.A.M. Theunissen, A.J. Burggraaf, Powder preparation and compaction behavior of fine-grained Y-TZP, J. Mater. Sci. 25 (1990) 3449–3455.
[43] M. Gaudona, E. Djurado, N.H. Menzler, Morphology and sintering behavior of yttria stabilized zirconia (8-YSZ) powders synthesized by spray pyrolysis, Ceram. Int. 30 (2004) 2295–2303.
[44] S.J. Guo, Theory of Powder Sintering, Metallurgy Industry Publishing Company, Beijing, 1998, p. 15 cited by [26].
[45] A. Bravo-Leon, Y. Morikawa, M. Kawahara, M.J. Mayo, Fracture toughness of nanocrystalline tetragonal zirconia with low yittria content, Acta Mater. 50 (2002) 4555–4562.
[46] S. Tekeli, The flexural strength, fracture toughness, hardness and densification behavior of various amount of Al_2O_3-doped 8YSCZ/Al_2O_3 composites used as an electrolyte for solid oxide fuel cell, Mater. Des. 27 (2006) 230–235.
[47] N.Q. Minh, Ceramic Fuel Cells, J. Am. Ceram. Soc. 76 (1993) 563–588.